A Wide-angle Broadband Converter: from Odd-Mode Spoof Surface Plasmon Polaritons to Spatial Wave

Hao Chi Zhang, *Member, IEEE*, Lin Liu, Pei Hang He, Jiayuan Lu, Le Peng Zhang, Jie Xu, Liangliang Liu, *Member, IEEE*, Fei Gao, Tie Jun Cui, *Fellow, IEEE*, Qijie Wang, *Senior Member, IEEE*, and Yu Luo

***Abstract*—A wide-angle broadband converter from odd-mode spoof surface plasmon polaritons (SPPs) to spatial wave is proposed based on gradual changed structure and Vivaldi shape flaring structure. We firstly demonstrate the dispersion, Eigen-mode and effective circuit topology of the designed spoof SPPs structure, which can support an odd mode as the propagated fundamental mode. A conversion structure between odd-mode spoof SPPs and spatial mode has been designed to implement smooth impedance and wavenumber transition. The optimized geometrical parameters are obtained through the full-wave simulation method and we fabricate this conversion structure using print circuit board (PCB) technology. Measured results from far field and near field both show that this structure has successfully excited odd mode spoof SPPs which come from an extremely wide-angle spatial radiation. The allowed azimuthal and pitched angle ranges are larger than 72 degrees.**

***Index Terms*—odd mode, surface plasmon polaritons, wide-angle, broadband, spatial wave, converser.**

I. Introduction

SPOOF surface plasmons (SPs) are a kind of special TM mode surface waves, which are designed to mimic the excellent features of natural SPs at optical frequencies. Those inheriting features, including field confinement and enhancement, will help to solve the contradiction of the small volume and high-Q factor in sensor design [1]. For natural SPPs, they rely on an interface between two kinds of mediums with opposite dielectric constants. A medium with positive dielectric constant is regarded as common dielectric. According to Drude model, the dielectric constant of a natural noble metal can be expressed as

$$\varepsilon_r(\omega) = 1 - \frac{\omega_p^2}{\omega(\omega + i\gamma)} \approx 1 - \frac{\omega_p^2}{\omega^2} \tag{1}$$

where the ω, ω_p and γ are the incident frequency, bulk plasmon oscillation frequency and damping factor of metal, respectively. Obviously, the dielectric constant of the metal will be negative if ω is smaller than ω_p. However, at microwave frequencies, the dielectric constant of metal will always be positive, which makes the metallic surface can only provide a very weak confinement of microwave energy.

To mimic the behavior of natural SPPs, 'structured metal' is proposed to provide negative dielectric constant in microwave band, such as the narrow meso-structure [2] and the periodic holes array [3]. The design rule of spoof SPPs is replacing the original oscillation of electrons in metal by the structured oscillation, which can reduce the metallic loss in optical band. Compared to natural SPPs-based devices, one of the most potential applications of spoof SPPs is to provide a solution for smaller loss devices (or high Q factors), for example, the spoof SPPs sensor [4]. Similar periodic structures have been investigated as slow-wave transmission structures or surface wave transmission structures based on the Floquet theorem since 1960s [5-8]. At microwave frequencies, these structures have been widely applied in power electronics, high-power microwave circuits, and CMOS technologies [9-11]. Laurette *et.al.* and Shen *et.al.* independently proposed an ultrathin structure to support spoof SPPs from the view of spoof SPP and planar surface wave transmission line (TL) [12-13]. Owing to the flexible and ultrathin features of this structure, it can be considered as a potential candidate of transmission line for flexible electronics. Inspired by this structure, there are many different structures are proposed to support the propagation of the spoof SPPs mode. Among them, the odd-mode spoof SPPs [14] waveguide can provide a more promising route to achieve anti-symmetrical subwavelength confinement compared to the common spoof SPPs. This is significant for some special

This work was supported in part from the National Science Foundation of China under Grant Nos. 61701246, 61631007, 61571117, 61501112, 61501117, 61522106, 61722106, 61701107, and 61701108, and 111 Project under Grant No.111-2-05., in part by Singapore Ministry of Education under Grant No. 2015-T1-001-117 (RG 72/15), and in part by National Research Foundation CRP Grant No. NRF2015NRF-CRP002-008.

Hao Chi Zhang, Lin Liu, Liangliang Liu, Qijie Wang and Yu Luo are with the School of Electrical and Electronic Engineering, Nanyang Technological University, Nanyang Avenue, 639798, Singapore (email: qjwang@ntu.edu.sg, luoyu@ntu.edu.sg)

Pei Hang He, Le Peng Zhang, Jiayuan Lu, Jie Xu, Wen Xuan Tang, and Tie Jun Cui are with State Key Laboratory of Millimeter Waves, Southeast University, Nanjing 210096, China and Synergetic Innovation Center of Wireless Communication Technology, Nanjing 210096, China (email: tjcui@seu.edu.cn).

Fei Gao is with the State Key Laboratory of Modern Optical Instrumentation, Zhejiang University, Hangzhou 310027, China.

Color versions of one or more of the figures in this paper are available online at http://ieeexplore.ieee.org.

Digital Object Identifier

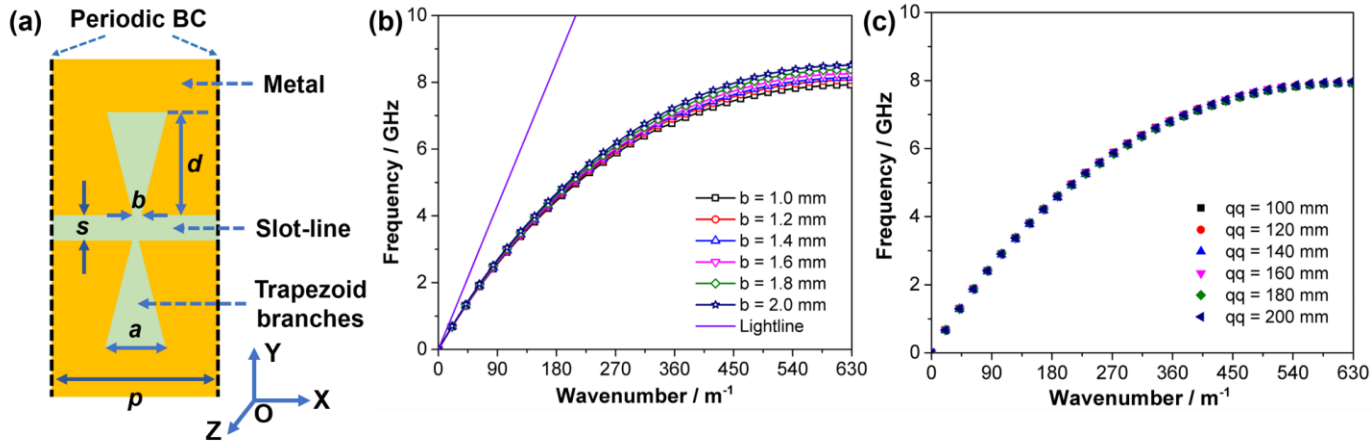

Fig. 1. The schematic diagram and dispersion curves of the odd-mode spoof SPPs. (a) the schematic diagram and geometrical parameter of the intact unit structure. (b) the dispersion curves of the odd-mode spoof SPPs with different base widths b, in which the period p = 5 mm, the slot width s = 0.25 mm, the bottom base width a = 2 mm and the height of the trapezoid branches d = 5 mm. (c) the dispersion curves of the odd-mode spoof SPPs with different distances between the structure and boundary qq, in which the period p = 5 mm, the slot width s = 0.25 mm, the bottom base width a = 2 mm, the base width b = 1mm and the height of the trapezoid branches d = 5 mm.

applications. For example, the differential transmission line. On the other hand, compared to the traditional odd-mode transmission line structure, the odd-mode spoof SPPs transmission line also has some useful features through properly designing SPP structure as the common spoof SPPs, such as smaller transmission loss [15-16], less bending loss [17], smaller packaging volume [18] and lower crosstalk [19-20].

Furthermore, some passive and active circuit devices are also constructed by taking the advantages of spoof SPPs [21-27]. Among these devices, antennas attract many attentions. Many kinds of SPP-excited antenna are reported, including the dielectric antenna [28], multibeam antenna [29], leakage mode antenna [30-32], and end-fire antenna [33]. However, all of them are designed based on even-mode spoof SPP transmission lines which are very difficult to excite odd-mode spoof SPPs. Hence, it is necessary to provide a solution to excite the odd-mode spoof SPPs.

However, a remarkable feature of spoof SPPs is that their dispersion curve deviates from the light-line in air, which implies that their momentums are mismatching with light. Hence, it is difficult to excite spoof SPPs directly based on the spatial wave radiating. A possible scheme to solve this problem is using couplers based on the metasurface [34-36]. But most of them are designed to excited spoof SPPs propagating on a two-dimensional (2D) surface rather than on a 1D waveguide which is widely used in the integrated circuit. Another limitation of those proposed meta-couplers is the narrow working band since the gradient phase array is constructed based on the resonance of metallic structures.

In this work, we proposed a new scheme to achieve smooth conversion between odd-mode spoof SPPs and spatial waves. The proposed structure is composed of three parts: 1) the flaring structure for conversion between spatial wave and slot line. It is similar to the Vivaldi antenna structure [37], which is a kind of broadband travel-wave antenna. 2) the gradually varied structure to achieve impedance conversion between the slot line and odd-mode spoof SPP TL. 3) the microstrip feed structure to receive the energy propagating in spoof SPPs waveguide. In fact, according to the Lorentz reciprocity theory, this structure can also work as an odd-mode spoof SPP antenna.

This paper is organized as follows. Firstly, the dispersion relation and field distribution of the complementary corrugated strips are investigated in Section II to verify this structure can support odd-mode spoof SPPs. Then, the smooth conversion structure between odd-mode spoof SPPs and spatial EM waves is presented in Section III. Section IV elaborates the fabricated sample of this broadband spatial wave converter, experimental setup and results of near- and far-field. Finally, we further

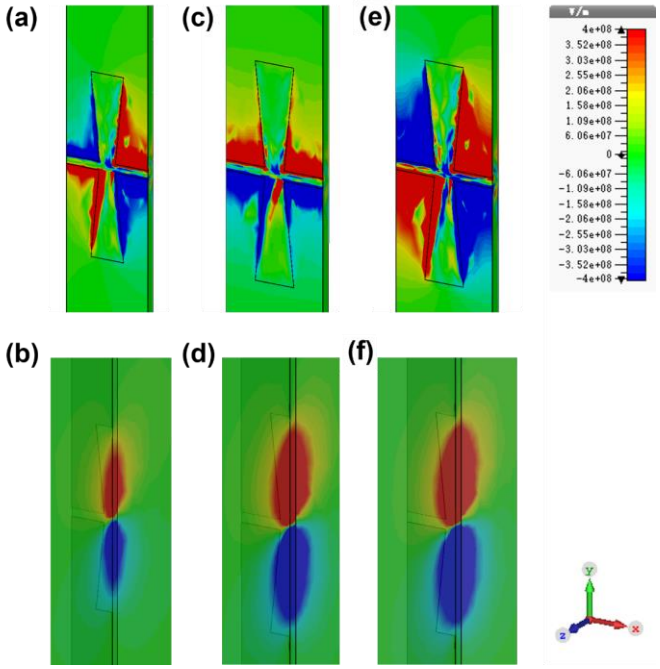

Fig. 2. The simulated Eigen-mode distribution of odd-mode spoof SPPs. (a-b) the z (a) and x (b) component of E-field distribution with 60-degree phase shift state. (c-d) the z (c) and x (d) component of E-field distribution with 120-degree phase shift state. (e-f) the z (e) and x (f) component of E-field distribution with 180-degree phase shift state.

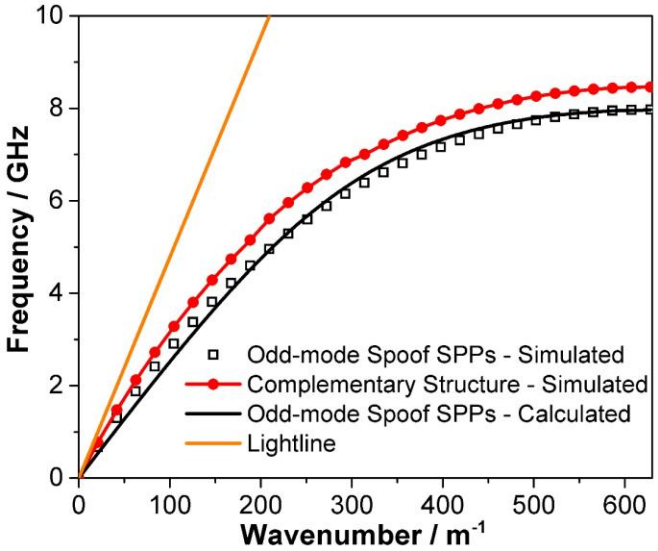

Fig. 3. The simulated and calculated results of the dispersion curves of the odd-mode spoof SPPs structure and its complementary structure.

discuss the advantages of this kind of spoof SPP converter and some potential applications in Section V.

II. Dispersion And Field Distribution Of Odd-Mode SPP Structure

In most cases, even-mode is the basis mode of the spoof SPPs-based circuit. We propose a kind of complementary spoof SPPs unit structure schematically shown in Figure 1(a), which consists of a slot line in the center and twin trapezoid branches. Here, the trapezoid branches are proposed to replace the rectangle branches in the previous design [33]. This provides an extra degree of freedom to control the field confinement, thereby helping us achieve stronger confinement using the structure within a fixed width. The dispersion curve of this structure with various base widths b is shown in Figure 1(b), while other parameters were chosen as the period p = 5 mm, the slot width s = 0.25 mm, the bottom base width a = 2 mm and the height of the trapezoid branches d = 5 mm. The metal and dielectric substrate are selected as the copper with 0.036 mm thickness and the Rogers RT 5880 with 0.508 mm thickness. The simulation is carried out by the Eigen-mode solver of the commercial software, CST Microwave Studio. Since this solver cannot support the open boundary, we set the electrical boundary around the spoof SPPs structure, and the distance between the structure and boundary qq is set as 100 mm which is about 2 times of the wavelength of the center frequency. To validate this method, we sweep the distance between the electric wall and the plasmonic surface ds from 100 mm to 200 mm with 20 mm step, and the dispersion curve is shown in Figure 1(c). It is clearly observed that these dispersion curves almost overlap, which implies that the eigen-mode simulation is stable. In addition, to accelerate the simulation, the loss of the metal and dielectric are ignored, which will lead to a tiny red shift of dispersion according to a previous study [19].

From Figure 1(b), it is clearly observed that all the dispersion curves of the spoof SPP structure with different base widths gradually deviate away from that of free space and slot structure.

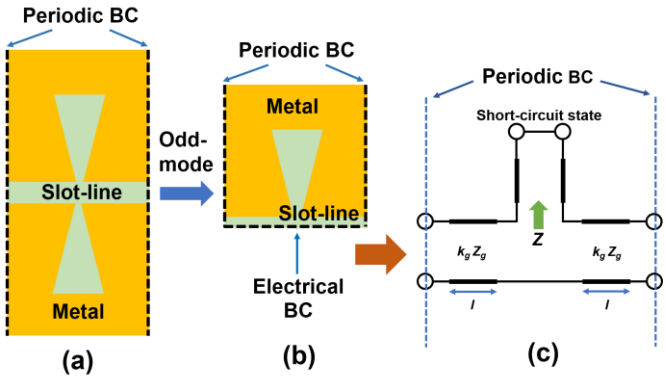

Fig. 4. The schematic diagram of the geometrical structure and effective circuit topology of the odd-mode spoof SPPs unit structure. (a) the schematic diagram of the intact unit structure. (b) the effective unit structure in case of the odd-mode propagation. (c) the effective circuit topology of the odd-mode spoof SPPs mode.

Meanwhile, dispersion curves of spoof SPPs structures with different base widths approaches different special cut-off frequencies as the wavenumber increases, which is similar to natural SPPs in optical frequency. We can also find that the dispersion curve of the structure with smaller width is lower than larger size one, which implies that the structure with smaller width can provide tighter field enhancement.

The field-distributions of the Eigen-mode of this structure at different phase shift states are shown in Figure 2. It can be observed that field is localized around the spoof SPP structure, which is the reason why the electrical boundary condition does not affect the dispersion curve. More importantly, the electric field is antisymmetric on the narrow slot. So, the basic mode of

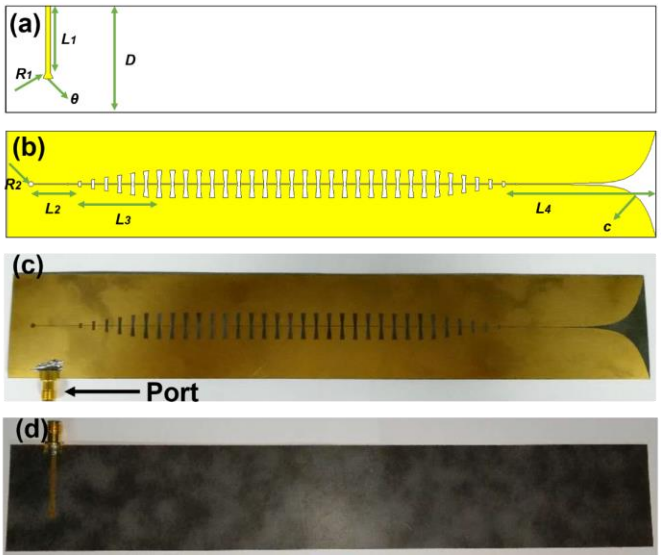

Fig. 5. The schematic diagram and the sample photos of conversion structure. (a) The front view of the schematic diagram of conversion structure, in which the length and width of feed line l_1 = 25.125 mm and w_1 = 1.8 mm, respectively, the radius and flare angle of the sector capacitance R_1 = 4.3 mm and $\theta = \pi/7$, respectively, and the width of the conversion structure D = 40.25 mm. (b) The bottom view of the schematic diagram of conversion structure, in which the radius of terminal R_1 = 1 mm, the distance between the slit and gradient structure l_2 = 12 mm, the length of the gradient structure l_3 = 34.5 mm, the length the exponential structure slit to l_4 = 50 mm, and the index of exponential structure c =4. (c) the front view of the sample photo of conversion structure. (d) The bottom view of the sample photo of conversion structure.

this structure is an antisymmetric odd mode. However, for the original structure [13], both the basic mode and the 1-st high-order mode are even modes, which is difficult to be excited with a high efficiency.

Then, we investigate the dispersion difference between the odd-mode spoof SPP structure and its complementary even-mode structure [38]. Figure 3 shows the simulated result of dispersion curves of these two structures, where the structural geometrical parameters are same as those in Figure 1(c). Dispersion curves of odd-mode and even-mode spoof SPP structures are quite similar with each other, which implies that these structures have similar dispersion property. Hence, it is possible to achieve similar functional spoof SPP-based devices based on the odd-mode structure and Babinet principle. Furthermore, the dispersion curve of the odd-mode spoof SPP is lower than that of the even-mode structure, which means the odd-mode spoof SPP structure can achieve tighter field confinement than the even-mode structure. Therefore, the odd-mode structure is more suitable for applications requiring field confinement, such as suppressing the crosstalk between adjacent TLs.

To make the designing more convenient, we investigate the effective circuit topology approximation of the odd-mode SPP structure. Different from the previous research on the effective circuit topology of the even-mode spoof SPPs structure [15], our scheme introduces not only lump elements but also the TL model to describe the dispersion and impedance behavior of the odd-mode spoof SPP TL. The reason for introducing the TL model is that the guide-wavelength is nearly twice of the structural period. If we only consider about lump elements, the subwavelength approximation will not be able to meet near the cut-off frequency and the circuit topology constructed will lead to the error of design.

According to odd-mode properties and network theory, the odd-mode spoof SPP TL unit can be simplified to the upper half structure with the electrical BC on the cross section, as shown in Figure 4(a) and 4(b). The narrow slot can be recognized as slot-line waveguide, whose dispersion and impedance have been analyzed [39]. And the trapezoid branch can be regarded as the series impedance Z, which is further described as the short-circuited impedance gradient TL, shown in Figure 4(c). Hence, the ABCD matrix of the unit of odd-mode spoof SPPs structure can be analytical described as

$$\begin{bmatrix} A & B \\ C & D \end{bmatrix} = \begin{bmatrix} \cos(k_g l) & jZ_g \sin(k_g l) \\ j\sin(k_g l)/Z_g & \cos(k_g l) \end{bmatrix} \begin{bmatrix} 1 & Z \\ 0 & 1 \end{bmatrix} \begin{bmatrix} \cos(k_g l) & jZ_g \sin(k_g l) \\ j\sin(k_g l)/Z_g & \cos(k_g l) \end{bmatrix}$$
$$= \begin{bmatrix} \cos(2k_g l) + jZ\sin(2k_g l)/2Z_g & jZ_g \sin(2k_g l) + Z(1+\cos(2k_g l))/2 \\ j\sin(2k_g l)/Z_g - Z(1-\sin(2k_g l))/2Z_g^2 & \cos(2k_g l) + jZ\sin(2k_g l)/2Z_g \end{bmatrix} \quad (1)$$

where k_g and Z_g are the wavenumber and impedance of the slot-line waveguide, respectively, and l is the equivalent length of the slot-line waveguide. In the above formula, we describe the shunt branch using lumped element Z. The lumped impedance Z can be regarded as the whole impedance of a more complex network, which can be used to consider the spatial dispersion of the structure by introducing the TL model. In this case, according to the case that impedance gradient, the series shunt impedance Z is calculated analytically as:

$$Z = jZ_c \tan(k_c d) \quad (2)$$

where k_c, Z_c and d are the wavenumber, average impedance, and equivalent length of the shunt branch, respectively. Due to the periodic property of the whole structure, the eigenvalues of the ABCD matrix of the periodic structure must be written in form of $\exp(-jk_x p)$ according to the Bloch theorem. Thus, we can derive the dispersion equation as:

$$\det\begin{bmatrix} A - e^{jk_x p} & B \\ C & D - e^{jk_x p} \end{bmatrix} = 0 \quad (3)$$

where k_x and p are the equivalent wavenumber and the period of the whole structure, respectively. After simplifications, the dispersion relation can be expressed as

$$\cos(k_x p) = \cos(2k_g l) + jZ\sin(2k_g l)/2Z_g \quad (4)$$

To verify this circuit topology, we calculate the dispersion curve of the odd-mode spoof SPP structure with the same geometrical parameters in the Figure 3 using the above formula. It is clearly observed that the calculated result matches well with the simulated result, which implies that the circuit topology has great accuracy.

The Bloch impedance of the structure can be calculated analytically as the following formula based on the symmetrical network topology.

$$Z_{in} = \sqrt{B/C} = Z_g \sqrt{\frac{2jZ_g \sin(2k_g l) + Z(1+\cos(2k_g l))}{2jZ_g \sin(2k_g l) - Z(1-\sin(2k_g l))}} \quad (5)$$

Notice that this Bloch impedance is relative to the location of the reference, but it also works as characteristic impedance in the subsequent designing.

Different from the effective circuit topology of original even-mode spoof SPP structure [40, 41], the one of odd-mode spoof

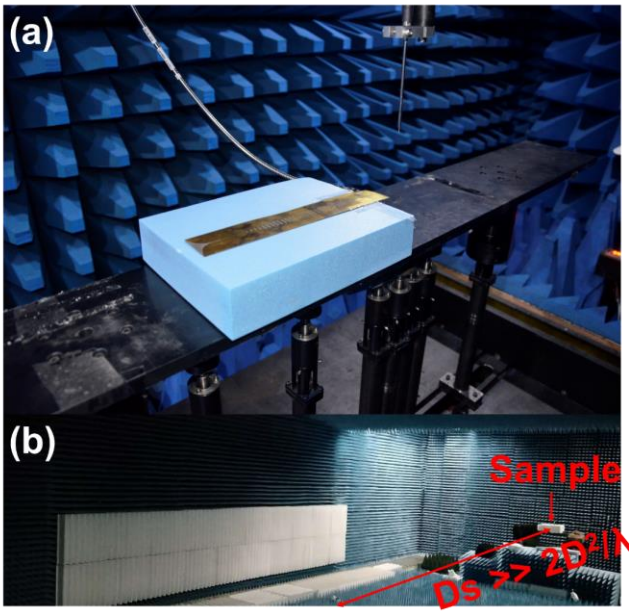

Fig. 6 The photograph for the near-field measurement (a) and the far-field measurement (b).

SPP structure is constructed by two transmission lines and a series dispersive inductance, rather than a paralleled dispersive capacitance. But considering from the dispersion formula, they are similar with each other based on the symmetry principle between electrical field and magnetic field. Hence, the odd-mode will not be affected by the terminal capacitance, which make the odd-mode can provide a strong field confinement, as predicted in Figure 3.

III. The Smooth Conversion Structure

As shown in Figure 1(b), the dispersion curves of the spoof SPP structure are under that of light, which means the momentum of spoof SPPs mismatches that of spatial EM waves. Therefore, spoof SPPs cannot be directly excited by free-spatial waves. Based on the discussion in introduction, the aim of our work is to provide a method to excite the spoof SPPs mode in a waveguide or transmission line (TL) rather than in a 2D surface. Thus, the intermediate structure should be a 1D waveguide structure rather than an array.

In order to achieve impedance and momentum matching, we utilize a slot structure as the bridge between the spoof SPPs and spatial wave mode. Considering the structure of odd-mode spoof SPP TL and slot line, conversion between them is easy by using the gradient trapezoid branches. Here, according to Figure 5(2) and (4), we can find that the cut-off frequencies can be controlled by the height d, which is similar to the properties of common spoof SPP structure [13]. Inspired by the conversion of the common spoof SPP structure [42], the smooth conversion is designed by gradually tuning the height of trapezoid branches d, as shown in Figure 5(a) and 5(b). The geometrical parameters of this unit is the same as in Figure 3 and other geometrical parameters are selected as the length of feeding line l_1 = 25.125 mm, the width of feeding line w_1 = 1.8 mm, the radius of the sector capacitance R_1 = 4.3 mm, the flare angle of the sector capacitance $\theta = \pi/7$, the width of the conversion structure D = 40.25 mm, the radius of terminal R_2 = 1 mm, the distance between the slit and gradient structure l_2 = 12 mm, the length of the gradient structure l_3 = 34.5 mm, the length the exponential structure slit l_4 = 50 mm, and the index of exponential structure c =4.

To achieve broadband and wide-angle conversion, it is required that both the impedance and momentum matches as broad as possible. Hence, it is impossible to use discontinuous structures, such as the 1/4 wavelength transformer section. Here, inspired by traveling wave antennas, we introduce the Vivaldi structure into the design to achieve the broadband conversion. A traditional conversion structure between the slot-line and microstrip [43] is used in our design.

To verify the performance of this device experimentally, we fabricated a sample using the print circuit board (PCB) technology, as shown in Figure 5 (c) and (d). In this figure, the main geometrical parameters are the same as those in simulation setup (i.e. Figure 5 (a) and (b)).

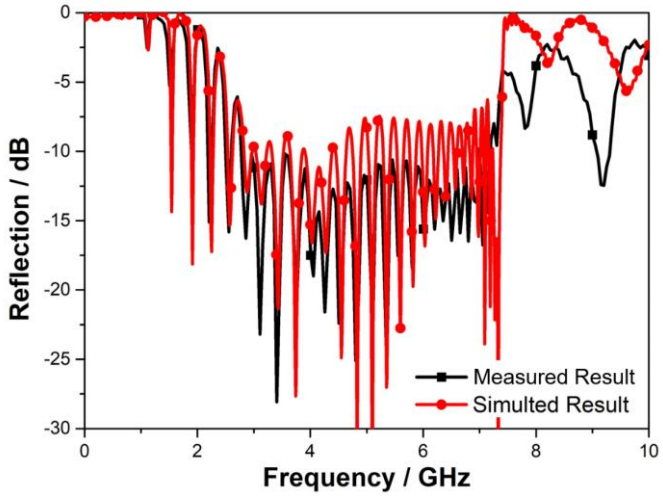

Fig. 7. The simulated and measured results of reflection coefficient of the conversion structure.

IV. The Method of Simulation and Experiment

According to the above discussion, three main properties of the converter should be investigated in the following simulations and experiments. Firstly, the odd-mode spoof SPPs is excited and propagating in the special designed spoof SPP waveguide. The wavenumber of this mode matches the calculated result of the circuit topology. Secondly, the broadband property of the converter should be achieved, which is easy to be verified by the simulated and measured S-parameters. Finally, the wide-angle performance of the converter can be realized and demonstrated by the far-field simulation and experiment. To demonstrate all the properties of the converter, the S-parameters measurement, near-field measurement and far-field measurement are necessary. To connect the sample with the measured equipment, we welded a common Sub-Miniature-A (SMA) connector to the terminal of the microstrip, which can make a smooth conversion between microstrip with 50 ohms and coaxial-cable with 50 ohms from 0 GHz to 17 GHz. Since it is a common operation to measure the S-parameter, we mainly introduce the method of the near-field and far-field measurement in this session.

A. Method of the simulation

The full-wave simulation of the converter is carried out by the time domain solver of the commercial software, CST Microwave Studio. Different from the Eigen-mode simulation, the metallic and dielectric loss are taken into consideration to ensure the veracity. The waveguide ports are set at the terminal of the conversion structure to excite the field in the slit. The BC is set as the open add space to mimic the free space. The E-field distribution and far field monitors are set from 3 to 7GHz by 1GHz step to obtain near-field and far-field results.

B. Method of the near-field measurement

The near-field distribution measurement is carried out by a home-made near-field scanner NFS001, which is placed in a microwave anechoic chamber to avoid the external interferential signal, as shown in Figure 6(a). The near-field

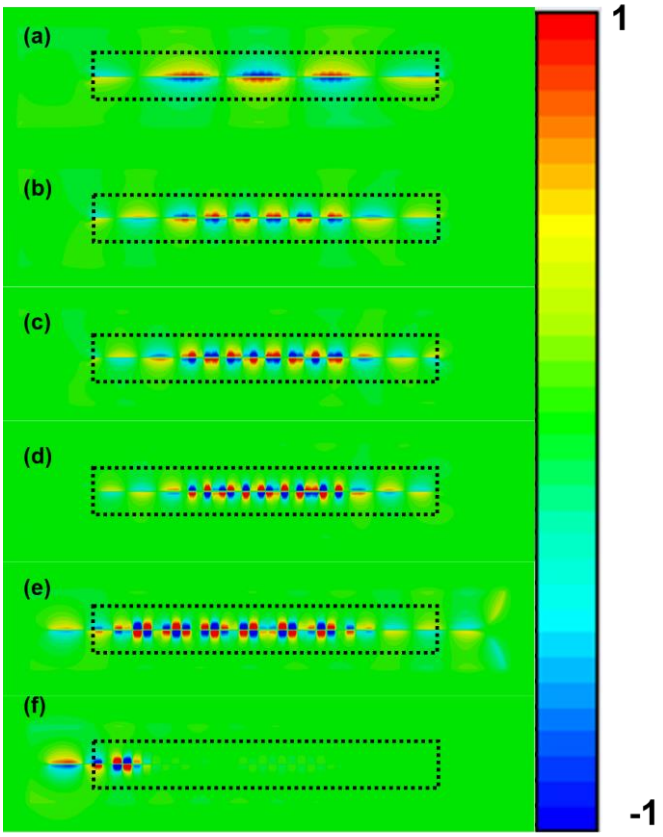

Fig. 8. The simulated near-field distribution of the structure at different frequencies. (a) 3 GHz; (b) 4 GHz; (c) 5 GHz; (d) 6 GHz; (e) 7 GHz; (f) 8 GHz.

scanner is composed of four parts: a two-port vector network analyzer (VNA) AV3672B, a bottom platform composed of the toughened bubble shell and the absorb materials, a monopole antenna installed in the upper platform as detector, a stepper motor which can move the antenna in *x*- and *y*-directions. Port #1 of the VNA is connected to the microstrip port to feed the converter. Port #2 of the VNA is connected to the receiving monopole antenna, which is fixed at 1 mm above the sample to detect the vertical z-component of electric field.

C. *Method of the far-field measurement*

The far-field measurement is placed in another microwave anechoic chamber. The sample connected to Port #1 of the VNA AV3672B is fixed on a rotary table, which is covered by absorb material, as shown in Figure 6(b). Port #2 is connected to a standard gain rectangular horn antenna, whose gain and efficiency have been standardized before. Meanwhile, the distance between the antenna and the sample satisfies the far field condition. To obtain the E-plane gain of the converter, the converter is horizontally placed on the rotary table. For the H-plane gain of the converter, the sample is vertically placed on the rotary table. In addition, the far-field of another standard gain rectangular horn antenna is measured as the reference to avoid the loss of free space.

V. The Simulated and Measured Results

Based on the measuring methods in the former section, we can obtain comprehensive simulated and measured results of the proposed converter. These results are shown in this section.

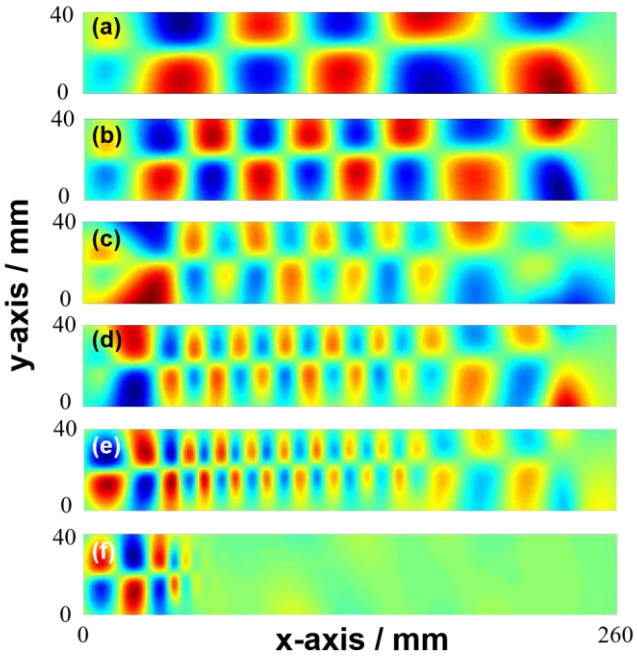

Fig. 9. The measured near-field distribution of the structure at different frequencies. (a) 3 GHz; (b) 4 GHz; (c) 5 GHz; (d) 6 GHz; (e) 7 GHz; (f) 8 GHz.

A. *Reflection coefficient of the conversion structure*

Reflection coefficient of this converter is shown in Figure 7. From this figure, we can find that the measured result matches well with the simulation, and both the simulated and experimental reflection coefficients of the conversion structure are lower than -10 dB from 3 GHz to 7 GHz. This implies that smooth conversion between the spoof SPP TL and space EM wave mode has been achieved. Note that the dielectric and metallic propagation loss are included in the measured result. However, owing to the low-loss feature of the dielectric substrate and copper in this band, most of the input energy are radiated into the air. Hence, considering the reciprocity of this device, the low reflection coefficient also implies that the device can be fed by spatial EM waves in a wide band.

B. *Near-field result of the conversion structure*

Simulated and measured near-field distribution results are presented in Figure 8 and 9, respectively, to demonstrate that the excited mode is an odd-mode SPP mode rather than other hybrid EM mode. Note that the near-field measurement is carried out in the area near the slit and branch structure, while the field is very weak in the other area.

In these figures, it is clearly observed that the E-field of this mode is antisymmetric, which implied that this EM mode is an odd mode. Meanwhile, the wavelength of this odd mode is compressed as predicted and the ratio of the wavelength compression varies with frequency rather than keeps constant. Another evidence for the existing of odd-mode spoof SPP mode is that the EM mode is cut off at the 8 GHz (i.e., the Figure 8(f) and 9(f)) as predicted in Figure. 3. Hence, the near-field

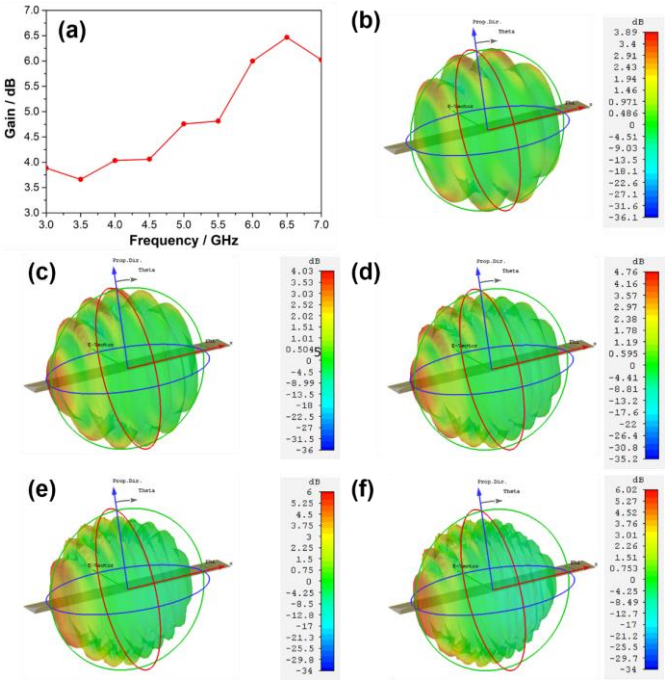

Fig. 10. The simulated gain diagram (a) and 3D gain directional diagram at different frequency; (b) at 3 GHz; (c) at 4 GHz; (d) at 5 GHz; (e) at 6 GHz; (f) at 7 GHz.

distribution results in Figure 8 and 9 provide a convincing demonstration for the propagation of odd-mode spoof SPPs.

C. Far-field result of the conversion structure

To verify the wide-angle feature, simulated and experimental far-field directional diagram are investigated to accurately evaluate the angle range of the converter. Simulated result of the gain-frequency diagram is shown in the Figure 10(a). We can find that the gain is about 5 dB and increases with the increase of frequency. This means the antenna keeps stable in this band. The increase of gain is a common phenomenon due to the equivalent radiation area increases with frequency. Simulated far-field and three dimensional (3D) gain directional diagram are displayed in Figure 11 (b-f). It is clearly observed that the main beam can scan most of the front space at different frequencies.

Efficiency is also an important index of the converter. Thus, we provide a simulated result of radiant efficiency and total efficiency of the converter. Radiant efficiency and total efficiency of this converter are about -0.5 dB -1.0 dB, respectively, in the band. Meanwhile, the declination of efficiency with the increase of frequency is caused by the loss enhancement at high frequencies.

In addition, we present measured E-plane and H-plane gain diagrams in Figure 11 (b-f) to quantitatively analyze the angle-range performance of this converter. From these figures, we find that the main beam can cover the range from -70 degrees to 70 degrees in azimuth and the range from -36 degrees to 36 degrees in elevation at the center frequency. Note that all the shapes of the far-field directional diagrams in the working band are very similar, which further reveals the broadband feature of the converter.

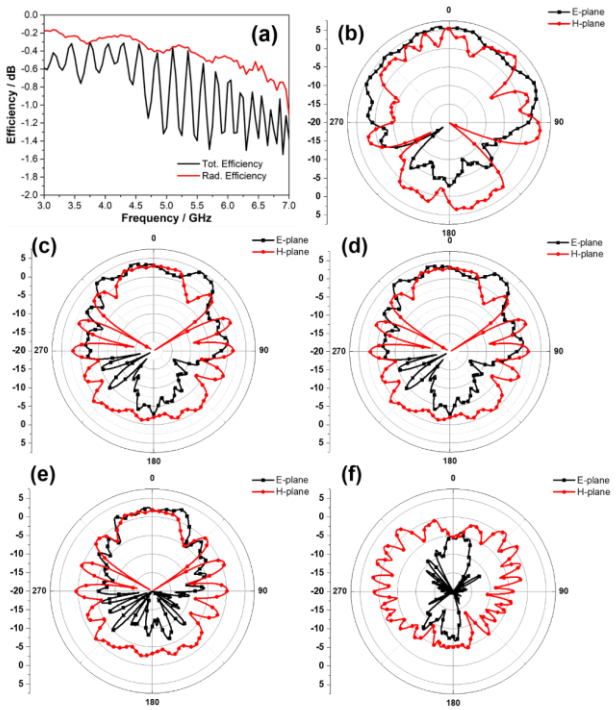

Fig. 11. The simulated efficiency diagram (a) and the measured E-plane and H-plane gain directional diagram at different frequency; (b) at 3 GHz; (c) at 4 GHz; (d) at 5 GHz; (e) at 6 GHz; (f) at 7 GHz.

VI. CONCLUSION

The dispersion behaviors of the narrow slot-line loaded the trapezoid branches structure, which has been demonstrated to support odd-mode spoof SPP mode as its fundamental mode, has been investigated. Effective circuit topology of the odd-mode spoof SPP structure is proposed to provide an approach to accurately design its dispersion property. Furthermore, inspired by the concept of traveling wave antenna, a broadband and wide-angle converter between odd-mode spoof SPPs and spatial waves is implemented to solve the problem of mode mismatching between these two kinds of modes. Propagation of odd-mode spoof SPP mode and its broadband and wide-angle features are demonstrated by the results of near-field scanning, reflection coefficient and far-field.

The proposed converter can be regarded as an antenna excited by odd-mode spoof SPPs as well. From the view of dispersion, odd-mode spoof SPPs can provide a general solution to reduce the length of feeder with constant phase shift, which is helpful to the miniaturization of devices.

ACKNOWLEDGMENT

H. C. Zhang, L. Liu, P. H. He and J. Lu contributed equally to this work. The authors would like to thank the Shanghai Shineshow Co., Ltd. for helping us design and build the near field scanner system NFS001.

REFERENCES

[1] J. N. Anker, W. P. Hall, O. Lyandres, N. C. Shah, J. Zhao, and R. P. Van Duyne, "Biosensing with plasmonic nanosensors," *Nature Materials*, vol. 7, pp.442-453, Jun. 2008.

[2] J. B. Pendry, A. J. Holden, W. J. Stewart and I. Youngs, "Extremely Low Frequency Plasmons in Metallic Mesostructures," *Phy. Rev. Lett.*, vol. 76, no. 25, pp. 4773-4776, Aug. 2004.

[3] J. B. Pendry, L. Martin-Moreno and F. J. Garcia-Vidal, "Mimicking surface plasmons with structured surfaces," *Science*, vol. 305, no. 5685, pp. 847-848, Aug. 2004.

[4] Z. Xu and P. Mazumder, "Bio-Sensing by Mach–Zehnder Interferometer Comprising Doubly-Corrugated Spoofed Surface Plasmon Polariton (DC-SSPP) Waveguide." *IEEE Trans. Terahertz Science and Technology*, vol. 2, no. 4 pp. 460-466, Jul. 2012.

[5] A. F. Harvey, "Periodic and guiding structures at microwave frequencies," *IRE Trans. Microw. Theory Tech.*, vol. 8, no. 1, pp. 30-61, Jan. 1960.

[6] A. A. Oliner and R. E. Collin, "*Field Theory of Guided Waves*," Hoboken, USA: Wiley-IEEE Press, 1991.

[7] W. Rotman, "A study of single-surface corrugated guides," *Proc. IRE*, vol. 39, no. 8, pp. 952-959, Aug. 1951.

[8] C. C. Culter, U.S. Patent 2 912 695, Nov. 10, 1959.

[9] K. Rawat and F. M. Ghannouchi, "A design methodology for miniaturized power dividers using periodically loaded slow wave structure with dual-band applications," *IEEE Trans. Microw. Theory Tech.*, vol. 57, no. 12, pp. 3380-3388, Dec. 2009.

[10] A.-L. Franc, E. Pistono, G. Meunier, D. Gloria, and P. Ferrari, "A lossy circuit model based on physical interpretation for integrated shielded slow-wave CMOS coplanar waveguide structures." *IEEE Trans. Microw. Theory Tech.*, vol. 61, no. 2, pp. 754-763, Feb. 2013.

[11] A. Niembro-Martín, V. Nasserddine, E. Pistono, H. Issa, A.-L. Franc, T.-P. Vuong, and P. Ferrari, "Slow-wave substrate integrated waveguide," *IEEE Trans. Microw. Theory Tech.*, vol. 62, no. 8, pp. 1625-1633, Aug. 2014.

[12] S. Laurette, A. Treizebre, and B. Bocquet, "Corrugated Goubau Lines to Slow Down and Confine THz Waves." *IEEE Trans. Terahertz Science and Technology*, vol. 2, no. 3, pp. 340-344, May. 2012.

[13] X. Shen, T. J. Cui, D. Martin-Cano, and F. J. Garcia-Vidal, "Conformal surface plasmons propagating on ultrathin and flexible films," *Proc. Natl. Acad. Sci. USA*, vol.110, pp. 40-45, Jan. 2013.

[14] X. Gao, L. Zhou and T. J. Cui, "Odd-Mode Surface Plasmon Polaritons Supported by Complementary Plasmonic Metamaterial." *Scientific Reports*, vol. 5. Mar. 2015, Art. ID: 9250.

[15] H. C. Zhang, Q. Zhang, J. F. Liu, W. Tang, Y. Fan and T. J. Cui, "Smaller-loss planar SPP transmission line than conventional microstrip in microwave frequencies," Scientific Reports, vol. 6, Mar. 2016, Art ID, 23396

[16] A. Kianinejad, Z. N. Chen and C. W. Qiu, "Design and modeling of spoof surface plasmon modes-based microwave slow-wave transmission line," *IEEE Trans. Microw. Theory Tech.*, vol. 63, no. 6, pp. 1817–1825, Jun. 2015.

[17] W. X. Tang, H. C. Zhang, J. F. Liu, J. Xu and T. J. Cui, "Reduction of radiation loss at small-radius bend using spoof surface plasmon polariton transmission line," Vol. 7, Jan. 2017, Art. ID, 41077.

[18] H. C. Zhang, W. Tang, J. Xu, S. Liu, J. F. Liu and T. J. Cui, "Reduction of Shielding-Box Volume Using SPP-Like Transmission Lines," *IEEE Transactions on Components, Packaging and Manufacturing Technology*, vol. 7, no. 9, pp. 1483-1490, May. 2017.

[19] W. Zhang, G. Zhu, L. Sun and F. Lin, "Trapping of surface plasmon wave through gradient corrugated strip with underlayer ground and manipulating its propagation," Appl. Phys. Lett. vol. 106, Jan. 2015. Art. ID: 021104.

[20] H. C. Zhang, T. J. Cui, Q. Zhang, Y. Fan, X. Fu, "Breaking the challenge of signal integrity using time-domain spoof surface plasmon polaritons," *ACS Photonics*, vol. 2, no. 9, pp. 1333−1340, Aug. 2015.

[21] H. C. Zhang, S. Liu, X. P. Shen, L. H. Chen, L. Li and T. J. Cui, "Broadband amplification of spoof surface plasmon polaritons at microwave frequencies," *Laser and Photonics Reviews*, vol. 1, no. 9, pp. 83-90. Nov. 2014.

[22] X. Liu, Y. Feng, K. Chen, B. Zhu, J. Zhao and T. Jiang, "Planar surface plasmonic waveguide devices based on symmetric corrugated thin film structures," *Optics Express*, vol. 22, pp 20107-20116, Aug. 2014.

[23] X. Gao, J. Shi, X. Shen, H. F. Ma, W. X. Jiang, L. Li and T. J. Cui, "Ultrathin dual-band surface plasmonic polariton waveguide and frequency splitter in microwave frequencies," *Applied Physics Letters*, vol. 102, no. 15, Apr. 2013, Art. ID: 151912.

[24] X. Shen, and T. J. Cui, "Planar plasmonic metamaterial on a thin film with nearly zero thickness," *Applied Physics Letters*, vol. 102, May. 2013, Art. ID: 211909.

[25] J. Y. Yin, J. Ren, H. C. Zhang, B. C. Pan and T. J. Cui, "Broadband frequency-selective spoof surface plasmon polaritons on ultrathin metallic structure," *Scientific Reports*, vol. 5. Feb. 2015, Art. ID: 8165.

[26] Q. Zhang, H. C. Zhang, H. Wu and T. J. Cui, "A hybrid circuit for spoof surface plasmons and spatial waveguide modes to reach controllable band-pass filters," Sc*ientific Reports*, vol. 5. Nov. 2015, Art. ID: 16531.

[27] X. Liu, Y. Feng, K. Chen, B. Zhu, J. Zhao and T. Jiang, "Planar surface plasmonic waveguide devices based on symmetric corrugated thin film structures," *Optics Express*, vol. 22, pp 20107-20116, Aug. 2014.

[28] A. Kianinejad, Z. N. Chen, L. Zhang, W. Liu, C.-W. Qiu, "Spoof Plasmon-Based Slow-Wave Excitation of Dielectric Resonator Antennas." *IEEE Trans. Antenna. Propag.* vol. 64, no.6, pp. 2094-2099. Jun. 2016.

[29] Y. Han, Y. Li, H. Ma, J. Wang, D. Feng, S. Qu, and J. Zhang, "Multibeam Antennas Based on Spoof Surface Plasmon Polaritons Mode Coupling." *IEEE Trans. Antenna. Propag.* vol. 65, no.3, pp. 1187-1192. Mar. 2017.

[30] J. Y. Yin, J. Ren, Q. Zhang, H. C. Zhang, Y. Q. Liu, Y. B. Li, X. Wan, and T. J. Cui, "Frequency-Controlled Broad-Angle Beam Scanning of Patch Array Fed by Spoof Surface Plasmon Polaritons." *IEEE Trans. Antenna. Propag.* vol. 64, no.12, pp. 5181-5189. Dec. 2016.

[31] A. Kianinejad, Z. N. Chen, and C.-W. Qiu, "A Single-Layered Spoof-Plasmon-Mode Leaky Wave Antenna With Consistent Gain." *IEEE Trans. Antenna. Propag.* vol. 65, no.2, pp. 681-687. Feb. 2017.

[32] Y. Fan, J. Wang, Y. Li, J. Zhang, S. Qu, Y. Han, and H. Chen, "Frequency-Scanning Radiation by Decoupling Spoof Surface Plasmon Polaritons via Phase Gradient Metasurface." *IEEE Trans. Antenna. Propag.* vol. 65, no.2, pp. 681-687. Feb. 2017.

[33] J. Y. Yin, D. Bao, J. Ren, H. C. Zhang, B. C. Pan, Y. Fan, and T. J. Cui, "Endfire Radiations of Spoof Surface Plasmon Polaritons." *IEEE Antennas And Wireless Propagation Letters*, vol. 16, pp. 597-600. 2017.

[34] W. Sun, Q. He, S. Sun, & L. Zhou, "High-efficiency surface plasmon meta-couplers: concept and microwave-regime realizations." *Light: Science & Applications*, vol. 5, no. 1, Jul. 2016, Art. ID: e16003.

[35] S. L. Sun, Q. He, S. Y. Xiao, Q. Xu, X. Li, & L. Zhou, "Gradient-index meta-surfaces as a bridge linking propagating waves and surface waves." *Nat. Mater.* vol. 11, pp. 426–431, May. 2012.

[36] J. J. Xu, H. C. Zhang, Q. Zhang & T. J. Cui, "Efficient conversion of surface-plasmon-like modes to spatial radiated modes." *Applied Physics Letters*, vol. 106, no. 2, Jan. 2015 Art. ID: 021102.

[37] S. Zhu, H. Liu, Z. Chen & P. Wen, "A compact gain-enhanced vivaldi antenna array with suppressed mutual coupling for 5g mm-wave application." *IEEE antennas and wireless propagation letters*, vol. 17, no. 5, pp. 776-779, May 2018.

[38] P. Wei, X. G. Guo, C. Zhang, R. Yang, Y. M. Zhu, "Groove-shape-induced bandwidth expansion of spoof surface plasmon polaritons on planar corrugated Goubau line in millimeter-wave range." *Optics Commun.* vol. 380, no. 1, pp. 352-356, Dec. 2016.

[39] P. Majumdar, A. K. Verma, "Integrated closed-form model and circuit model of lossy slot line." *IET Microw. Antennas Propag.*, vol. 5, no. 14, pp. 1763–1772, Aug. 2011.

[40] H. C. Zhang, T. J. Cui, J. Xu, W. Tang, and J. F. Liu, "Real-Time Controls of Designer Surface Plasmon Polaritons Using Programmable Plasmonic Metamaterial," *Advanced Materials Technologies*, vol. 1, Nov. 2016. Art. ID: 1600202

[41] H. C. Zhang, P. H. He, W. X. Tang, Y. Luo, and T. J. Cui, "Planar spoof SPP transmission lines and their applications in microwave circuits," *IEEE Microw. Mag.* Accepted. 2018.

[42] H. F. Ma, X. Shen, Q. Cheng, W. X. Jiang, and T. J. Cui, "Broadband and high-efficiency conversion from guided waves to spoof surface plasmon polaritons," *Laser. Photon. Rev.*, vol. 8, no. 1, pp. 146–151, Nov. 2016.

[43] D. Cao, Y. Li, and J. Wang, "Wideband compact slotline-to-spoof-surface plasmon-polaritons transition for millimeter waves." *IEEE antennas and wireless propagation letters*, vol.16, pp. 3143 – 3146, Oct. 2017.

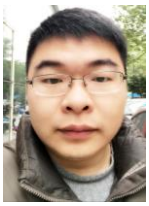

Hao Chi Zhang (S'15-M'18) was born in Jiaxing, Zhejiang, China, in 1991. He received the B.Eng. degree in electrical engineering from the University of Electronic Science and Technology of China, Chengdu, China, in 2013. He is currently immediately achieving the Ph.D. degree in electromagnetic and microwave technology from Southeast University, Nanjing, China. Now, He is currently at school of electrical and electronic engineering of Nanyang technological university, Singapore, as a project officer. His current research interests include microwave and millimeter-wave circuits and antennas technology, surface plasmons, and metamaterials. He has authored over 30 international refereed journal papers, in highly ranked journals, including Laser and Photonics Review, ACS Photonics, IEEE Transactions on Antenna and Propagation, Applied Physics Letters, etc.

Lin Liu received her B.Sc. degree in electronic information science and technology from Nanjing University, China, in 2015, and M.Sc. degree in electronics from Nanyang Technological University, Singapore, in 2016. She is currently pursuing her Ph.D. degree in Nanyang Technological University, Singapore. Her research interests include surface plasmonic polaritons (SPPs), metamaterials and light-matter interactions.

Pei Hang He received the B.S. degree from University of Electronic Science and Technology of China (UESTC), Chengdu, China, in 2017. He is currently pursuing the M.S. degree in Southeast University, Nanjing, China. His research interests include surface plasmonic polaritons (SPPs), metamaterials and millimeter waves theories and technologies.

Jiayuan Lu received the B.S. and M.S degree in electronics and information engineering from Nanjing University of Science and Technology, China, in 2014 and 2017 separately. He is currently working toward the Ph.D. degree in electromagnetic field and microwave technology in southeast university. His research interest is the design of miniaturized high-performance microwave / millimeter-wave passive device, surface plasmon and metamaterials.

Jie Xu received the B.S., M.S. and Ph. D. degrees in electrical engineering from Southeast University, Nanjing, China, in 2008, 2011 and 2017, respectively. In January 2018, he joined the School of Information Science and Engineering, Southeast University, Nanjing, China as a postdoctor.
His research interests include microwave and millimeter-wave circuits, metamaterial structures, and antennas design.

Liangliang Liu was born in Jiangsu, China, in 1987. He received the B.S. degree in information engineering, M.E. degree in electromagnetic field and microwave technology, and Ph.D. degree in communication and information system from Nanjing University of Aeronautics and Astronautics, China, in 2010, 2013 and 2017, respectively. He has authored or co-authored over 40 papers in international refereed journals and conference proceedings. He is currently at school of electrical and electronic engineering of Nanyang technological university, Singapore, as a Research Fellow. His current research interests include spoof surface plasmon polaritons, spoof localized surface plasmons, and metasurfaces.

Fei Gao received his B.Sc in Applied physics from Sichuan University, China, and M.Sc in Condensed Matter Physics from Nanjing University, China, in 2007 and 2010 respectively. From 2010 to 2012, he worked as a research assistant in Shenzhen Institute of Advanced Technology, Chinese Academy of Science. In 2016, Fei Gao received his Ph.D degree in Physics & Applied Physics from Nanyang Technological University, Singapore. From 2016 to 2018, Fei Gao became a Research Fellow in Nanyang Technological University, Singapore. In 2018, he joined the Department of Electrical Engineering in Zhejiang University, and hold a tenure-track position. Dr. Gao has published over 40 peer-review journal papers in Nature Physics, Nature Communications, Advanced Materials, Advanced Functional Materials, Laser & Photonics Review, etc. His research interests include metamaterials, topological electromagnetics, photonic crystals, acoustic crystals, photon-phonon interactions. In 2018, Dr. Gao was selected in Young 1000 Talents Plan.

Tie Jun Cui (M'98–SM'00–F'15) received the B.Sc., M.Sc., and Ph.D. degrees in electrical engineering from Xidian University, Xi'an, China, in 1987, 1990, and 1993, respectively. In March 1993, he joined the Department of Electromagnetic Engineering, Xidian University, and was promoted to an Associate Professor in November 1993. From 1995 to 1997 he was a Research Fellow with the Institut fur Hochstfrequenztechnik und Elektronik (IHE) at the University of Karlsruhe, Germany. In July 1997, he joined the Center for Computational Electromagnetics, Department of Electrical and Computer Engineering, University of Illinois at Urbana-Champaign, first as a Postdoctoral Research Associate and then a Research Scientist. In September 2001, he became a Cheung-Kong Professor with the Department of Radio Engineering, Southeast University, Nanjing, China. From 2013, he has been a Representative of People's Congress of China. Dr. Cui is the first author of the books *Metamaterials – Theory, Design, and Applications* (Springer, Nov. 2009) and *Metamaterials: Beyond Crystals, Noncrystals, and Quasicrystals* (CRC Press, Mar. 2016). He has published over 400 peer-review journal papers in Science, PNAS, Nature Communications, Physical Review Letters, Advanced Materials, IEEE Transactions, etc. His research interests include metamaterials, computational electromagnetic, wireless power transfer, and millimeter wave technologies, which have been cited by more than 16900 times (H-Factor 66). According to ELSEVIER, he is one of the Most Cited Chinese Researchers. Dr. Cui was awarded a Research Fellowship from the Alexander von Humboldt Foundation, Bonn, Germany, in 1995, received a Young Scientist Award from the International Union of Radio Science (URSI) in 1999, was awarded a Cheung Kong Professor under the Cheung Kong Scholar Program by the Ministry of Education, China, in 2001, received the National Science Foundation of China for Distinguished Young Scholars in 2002, received Special Government Allowance awarded by the Department of State, China, in 2008, received the Award of Science and Technology Progress from Shaanxi Province Government in 2009, was awarded by a May 1st Labour Medal by Jiangsu Province Government in 2010, received the First Prize of Natural Science from Ministry of Education, China, in 2011, and received the Second Prize of National Natural Science, China, in 2014. Dr. Cui's researches have been selected as one of the "Optics in 2016" by Optics and Photonics News Magazine (OSA), "10 Breakthroughs of China Optics in 2016", "10 Breakthroughs of China Science in 2010", "Best of 2010" in New Journal of Physics, Research Highlights in Europhysics News, Journal of Physics D: Applied Physics, Applied Physics Letters, and Nature China. His work has been reported by Nature News, Science, MIT Technology Review, Scientific American, New Scientists, etc.
Dr. Cui is an IEEE Fellow, and active reviewer for Science, Nature Materials, Nature Photonics, Nature Physics, Nature Communications, Physical Review Letters, Advanced Materials, and a series of IEEE Transactions. He was an Associate Editor in IEEE Transactions on Geoscience and Remote Sensing and a Guest Editor in Science China – Information Sciences. He served as an Editorial Staff in IEEE Antennas and Propagation Magazine and is in the editorial boards of Progress in Electromagnetic Research (PIER) and Journal of Electromagnetic Waves and Applications. He served as General Co-Chair of the International Workshops on Metamaterials (META'2008, META'2012), TPC Co-Chair of Asian Pacific Microwave Conference (APMC'2005) and Progress in Electromagnetic Research Symposium (PIERS'2004).

Qijie Wang (M'10–SM'10) received the B.E. degree in electrical engineering from the University of Science and Technology of China, Hefei, China, in 2001, graduating one year in advance, and the Ph.D. degree in electrical and electronic engineering from Nanyang Technological University (NTU), Singapore, in 2005, with NTU and Singapore Millennium Foundation (SMF) scholarship. He received the 2005 SMF Post-Doctoral Fellowship at NTU. In 2007, he joined the School of Engineering and Applied Science, Harvard University, as a Postdoc-toral Researcher. In 2009, he was assigned as a Joint Nanyang Assistant Professor in the Microelectronics Division, School of Electrical and Electronic Engineering, and in the Physics and Applied Physics Division, School of Physical and Mathematical Sciences. In 2018, he was promoted to Professor in the same school. His current research interests are to explore theoretically and experimentally nanostructured semiconductor and fiber-based materials, and nanophotonic devices (nanoplasmonics, photonic crystals, and metamaterials) with an emphasis on all aspects of the problem from design, fabrication, and characterization to integration at system level.
Dr. Wang received the top prize for the Young Inventor Awards of the SPIE Photonics Europe Innovation Village in 2004, a golden award from the Fifth Young Inventor's Awards from HP and Wall Street Journal in 2005, the Institution of Engineers Singapore Engineering Achievement Team Award in 2005 and 2017 respectively, and the Singapore Young Scientist Award 2014.

Yu Luo received the B.E. degree in electronic and information engineering from Zhejiang University, Hangzhou, China, in 2006, and the Ph.D. degree in physics from Imperial College London, London, U.K., in 2012. He was with Imperial College London, as a Research Associate. In 2015, he joined the School of Electrical and Electronic Engineering, Nanyang Technological University, Singapore, as an Assistant Professor. He has been involved in a wide range of topics within the realm of metamaterials and plasmonics ranging from the design of invisibility cloaks and plasmonic light-harvesting devices to the study of nonlocal and quantum phenomena in mesoscopic plasmonic systems. He has authored over 60 international refereed journal papers, which have received over 2000 citations.